Stable High Beta Plasmas Confined by a Dipole Magnetic Field

D. T. Garnier,* A. Hansen, M. E. Mauel, and E. Ortiz

Department of Applied Physics and Applied Mathematics

Columbia University, New York, NY 10027

A. Boxer, J. Ellsworth, I. Karim, J. Kesner, S. Mahar, and A. Roach

Plasma Science and Fusion Center, MIT, Cambridge, MA 02139

(Dated: October 20, 2005)

Abstract

Stable high-beta plasma is created and confined by the magnetic field of a superconducting coil that is suspended within a large vacuum chamber by thin supports. Discharges containing trapped electrons form when microwaves cause strong perpendicular heating at cyclotron resonance. At low gas fueling rates, an instability appears that resonates with the magnetic drifts of fast electrons and causes rapid radial transport. Higher gas fueling stabilizes the instability and allows the fast electron pressure to rise until the ratio of plasma to magnetic pressure, $\beta \equiv 2\mu_0\, p/B^2$, attains 20%.

PACS numbers: 52.55.-s, 52.50.SW, 52.35.-g

The levitated dipole experiment (LDX), shown in Fig. 1, is a new research facility that was designed to investigate the confinement and stability of plasma in a dipole magnetic field configuration [1]. The dipole confinement concept was motivated by spacecraft observations of planetary magnetospheres that show centrally-peaked plasma pressure profiles forming naturally when the solar wind drives plasma circulation and heating [2]. Unlike most other approaches to magnetic confinement in which stability requires average good curvature and magnetic shear, MHD stability in a dipole derives from plasma compressibility [3–5]. Plasma is stable to interchange and ballooning instabilities when the pressure gradient is sufficiently gentle even when the local plasma pressure exceeds the magnetic pressure or, equivalently, when $\beta \equiv 2\mu_0\, p/B^2 > 1$ [6]. In this letter we report the first production of high beta plasma confined by a laboratory dipole using neutral gas fueling and electron cyclotron resonance heating (ECRH). The pressure results from a population of energetic trapped electrons that can be maintained for many seconds of microwave heating provided sufficient neutral gas is supplied to the plasma.

A number of previous experiments also used ECRH to produce high beta plasma [7–10]. Energetic trapped electrons were first generated in the ELMO experiments [7] where harmonic cyclotron absorption created a localized "ring" of weakly relativistic electrons ($E_h \sim 400$ keV) within a plasma containing a larger density of cooler electrons. Linked magnetic mirrors, in which high beta electron rings were created, formed the bumpy torus device [8]. In simple axisymmetric mirrors, internal magnetic probes were able to characterize the plasma equilibrium, and, during optimal conditions, multiple-frequency ECRH [9] produced anisotropic plasmas that reached high values of local beta, $\beta \approx 40\%$, and high ratios of the perpendicular and parallel pressures, $\beta_\perp/\beta_{||} \approx 4.3$. A similar study using a non-axisymmetric, minimum-B, magnetic mirror [10] also achieved $\beta \approx 35\%$ with weakly relativistic electrons having anisotropic pressure $\beta_\perp/\beta_{||} \gg 1$.

The observations of stable high beta electron plasmas confined by axisymmetric mirrors are noteworthy because the pressure gradients exceeded the usual criteria for MHD stability. Stability was possible because instabilities driven by fast electrons acquire a real frequency, $\omega \approx m\omega_{dh}$, proportional to the product of the azimuthal mode number, m, and the magnetic drift frequency of the fast electrons. The real frequency induces a stabilizing ion polarization current [11, 12] that imposes an instability threshold inversely proportional to the ratio of the line-averaged fast electron and ion densities, $\bar{n}_h/\bar{n}_i$. The high-frequency

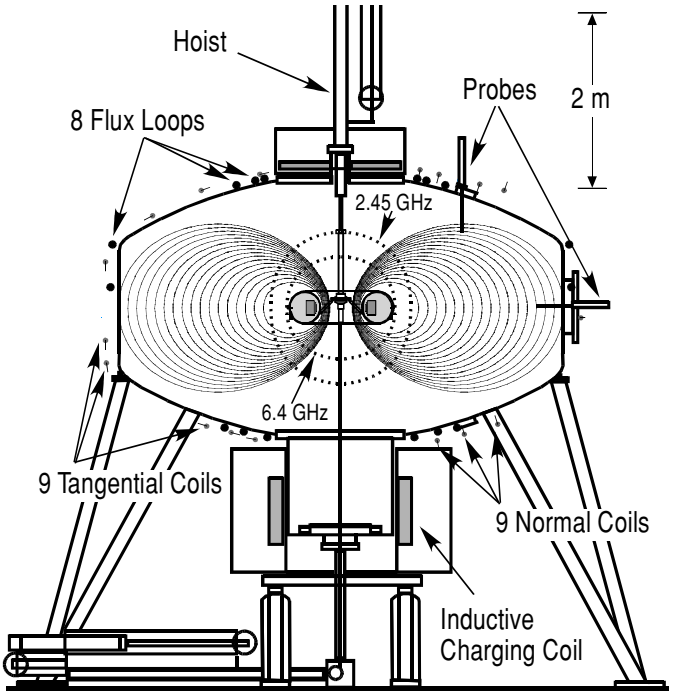

FIG. 1: Schematic of LDX experiment showing the dipole magnet suspended within the vacuum vessel. Loops and coils measure the equilibrium plasma current, and probes measure fluctuating potentials. Injected microwave power strongly heats electrons at the cyclotron resonance.

hot electron interchange (HEI) instability [12] has a mode number, $m \sim 7$, and a real frequency above the ion cyclotron frequency, $\omega \approx m\omega_{dh} > \omega_{ci}$. This mode was observed in bumpy tori, and it destroyed fast electron confinement when $\bar{n}_h/\bar{n}_i \sim 40\%$ [13]. The low-frequency HEI instability, first described by Krall [11], was predicted to occur when $-d\ln(\bar{n}_h V)/d\ln V > (m_\perp^2/24)\,(\omega_{dh}/\omega_{ci})\,(\bar{n}_i/\bar{n}_h)$, where V is the differential volume of a magnetic flux tube and $m_\perp$ is a total perpendicular wavenumber [14]. The low-frequency HEI was observed in low beta plasma, $\beta < 1\%$, containing energetic electrons trapped in a supported dipole experiment [15, 16]. In the low beta dipole experiment, the HEI appeared with low azimuthal mode number, $m \sim 1$, a broad radial mode structure, and a complex, time-evolving frequency spectrum [16]. Intense bursts of instability induced chaotic radial transport [15], and nonlinear frequency-sweeping was evidence for the inward propagation of "phase-space holes" [17].

In the experiments reported here, the trapped electron beta was also limited by the low-frequency HEI, but when the neutral gas was programmed so as to maintain the deuterium gas pressure between about 1-3 $\times 10^{-6}$ Torr, the fast electron pressure increased by more

than a factor of ten and the stable high beta plasma could be maintained for many seconds. The high beta plasma generated a large equilibrium toroidal current, $I_p > 3$ kA, that is analogous to the ring current generated by high beta plasma in the Earth's magnetosphere [18]. Measurements of magnetic field of the plasma current and the location of fast electrons using x-ray imaging constrain models for the anisotropic pressure profile and allow estimates of the plasma stored energy, $W_p > 300$ J, and peak beta, $\beta \approx 20\%$. We also find the presence of instability creates hysteresis in high-beta plasma behavior. High neutral fueling is required to create a high beta plasma, but, once stabilized, lower neutral fueling is needed to maintain the high beta state.

As shown in Fig. 1, LDX consists of an internal superconducting coil located within a 5 m dia. vacuum chamber. The coil's dipole moment is $M = 0.34\, I_d$ A·m^2, and experiments have been conducted with $I_d = 1.2$ MA. A large bore superconducting coil, located below the main chamber, is used to inductively charge the dipole coil. The dipole is lifted for plasma experiments by a vacuum hoist. In this configuration three 1.5 cm dia. support rods intersect the plasma causing heat and particles to be lost from the plasma. (In future experiments the coil will be magnetically levitated, eliminating losses to the support rods.) Plasma diagnostics include 26 magnetic sensors to detect the plasma equilibrium current, probes to measure electrostatic fluctuations and edge plasma parameters, x-ray and visible light imaging cameras, and a microwave interferometer to measure the line-averaged plasma density.

Fig. 2 shows diagnostic signals from a typical LDX high-beta discharge. 5 kW of total ECRH microwave power was applied to the plasma with equal amounts from 2.45 GHz and 6.4 GHz sources. The deuterium pressure was adjusted with four pre-programmed gas puffs. After an initial period lasting 0.25 s, the light emitted from the plasma abruptly increases followed by a more gradual increase in the perturbed magnetic flux near the outer equator. Since this detector senses 0.78 mV·s/kA for a current ring located at 1 m radius, Fig 2 indicates several kA of equilibrium plasma current. Measurements using a microwave interferometer show the light emission is roughly proportional to the plasma line-density. By viewing the dipole magnet from several directions, we know x-rays result from plasma bremsstrahlung and from fast electrons driven inward to the dipole magnet. When the ECRH power is switched-off, the plasma equilibrium current slowly decays proportional to the collisional loss rate of the trapped electrons.

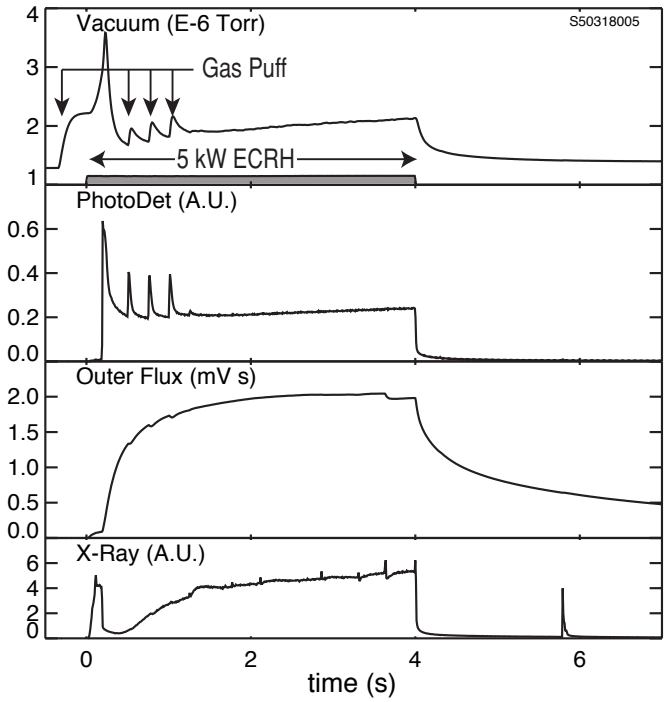

FIG. 2: Example high beta plasma discharge created with 5 kW ECRH power and four gas puffs. Measurements show (i) the deuterium gas pressure within the chamber, (ii) the visible light from the plasma, (iii) the magnetic flux near the outer equator, and (iv) the x-ray intensity.

The radial location of the fast electron population is viewed by an x-ray camera during times when the ECRH is on and by a visible camera that detects the ionization glow of the trapped electrons after the microwave heating pulse ends. The x-ray camera contains a medical x-ray image intensifier sensitive to energies greater than 45 keV that was previously used during tokamak heating experiments [19]. A standard video camera is used to observe the fast electrons during the afterglow as described in Ref. [10]. For single-frequency ECRH, the cameras indicate the pressure peak is localized on the equatorial plane of the fieldlines having the fundamental cyclotron resonance at the minimum B. This is expected for ECRH since electrons mirror-trapped at resonance are continuously heated by the injected microwaves [20, 21]. When both 2.45 GHz and 6.4 GHz sources are on, the x-ray image shows the fast electrons localized at the equator but spanning both resonances in the radial direction.

Estimates of the plasma pressure are made by computing the least-squares best-fit of a model to the magnetic diagnostics. We use an anisotropic pressure profile, with $P_\perp > P_{||}$,

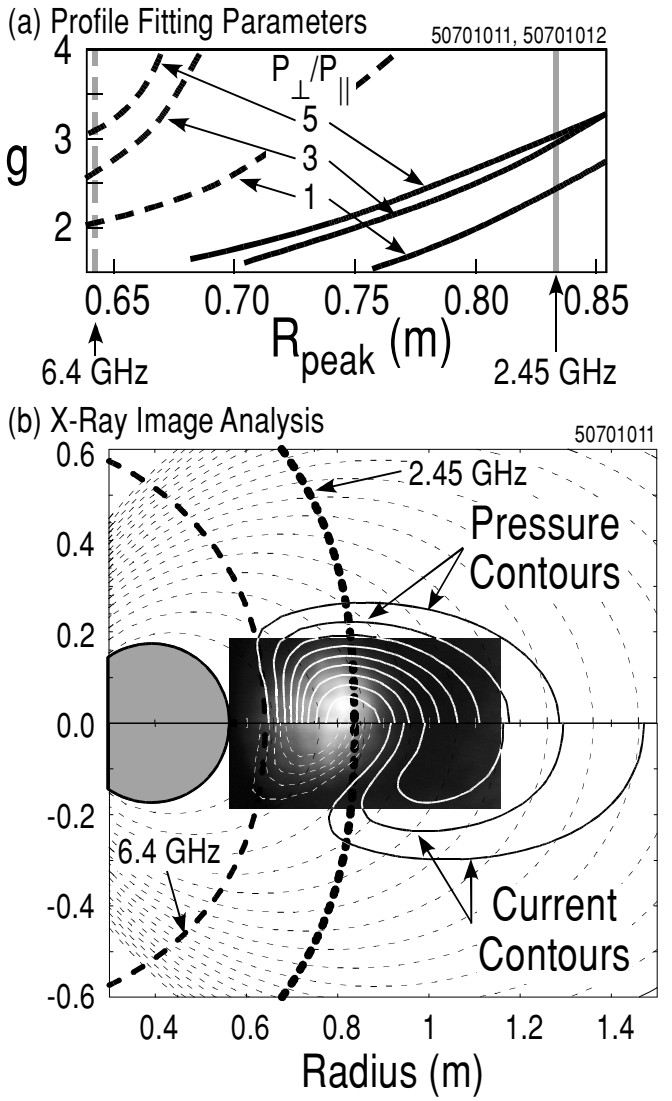

FIG. 3: Profile parameters and contours of pressure and current that best fit magnetic measurements for discharges with single-frequency ECRH. X-ray image shows localization of fast-electrons.

that is similar to that used to study plasma equilibrium and stability in the magnetic field of a point dipole [22, 23] and given by $P_\perp(\psi, B) = \hat{P}(\psi)(B_0(\psi)/B)^{2p}$ where $\mathbf{B} = \nabla\phi \times \nabla\psi/2\pi$ and $B_0(\psi)$ is the minimum field strength on a field-line. With this model, the ratio of perpendicular to parallel pressure is a constant, $P_\perp/P_{||} = 1 + 2p$. To fit this model to the magnetic measurements, the plasma current, $J_\phi(r, z)$ is related to the pressure through the self-consistent equilibrium, $\psi(r, z)$. However, since the dipole moment of J_ϕ is less than 2% of the coil's magnetic moment, the difference between J_ϕ computed using the vacuum dipole field and the self-consistent field is undetectable for the beta achieved to date. Using

the dipole's vacuum field, the plasma ring current density can be computed from any given function of $\hat{P}$ and parameter p using $J_\phi = -2\pi r\,[D_\psi P_\perp + 2pP_\perp D_\psi \ln B/(1+2p)]$, where $D_\psi \equiv |\nabla\psi|^{-2}\nabla\psi\cdot\nabla$. The detected signal from a magnetic sensor is computed by combining contributions from J_ϕ throughout the plasma with the decrease of I_d required to maintain constant the flux linked by the superconducting dipole. For the reconstructions reported here, $\hat{P} = \Delta(\psi) \times P_0(\psi/\psi_0)^{4g}$, where $\Delta(\psi) = [(\psi-\psi_d)/(\psi_0-\psi_d)]^\alpha$ is chosen to vanish at the surface of the dipole, ψ_d, and to equal unity at the location of the pressure peak, ψ_0. Far from the coil's surface, $|\psi| \ll |\psi_d|$, the equatorial pressure is $P_\perp(r) \approx P_0(R_{peak}/r)^{4g}$. This form resembles the MHD condition for marginal stability, expressed as $\delta(PV^\gamma) = 0$ with $\gamma = 5/3$, that is equal to $P \sim r^{-4\gamma}$ in a dipole [3–6, 23].

Fig. 3 illustrates the model pressure and current profiles that are the least-squares best fit to the magnetic measurements of high beta plasma produced with single-frequency ECRH. We find equally good fits occur either with steep profiles centered at large radii or with broad profiles centered at smaller radii. This results because J_ϕ is primarily determined from the pressure gradient and the magnetic sensors are most sensitive to the plasma's dipole moment. When only 2.45 GHz heating is applied (solid lines in Fig. 3a), very good fits result with $1.7 < g < 3.1$ when $0.68 < R_{peak} < 0.85$. Because we observe the fast-electron population to peak at the ECRH resonance, $R_{peak} = 0.83$ m, we conclude $g = 2.0,\ 2.8,\ 3.1$ for $p = 0,\ 1,\ 2$, respectively. When only 6.4 GHz microwaves are applied, $R_{peak} = 0.64$ m, and $g = 2.0,\ 2.8,\ 3.5$ for $p = 0,\ 1,\ 2$. Because of the dipole support rods, $p > 0$. From this, previous experiments [9, 10], and the measured height of the x-ray images, we believe the pressure is well approximated by $P_\perp/P_{||} \sim 5$. Fig. 3b show the model $P_\perp$ and J_ϕ profiles that best fit measurements.

Plasma with the highest values of I_p and β are created with both 2.45 GHz and 6.4 GHz heating. The sum of the mean-square deviations between the best-fit model profile and the magnetic measurements doubles as compared with single-frequency heating, and this may be related to the presence of two pressure peaks, one at each resonance. If R_{peak} is assumed to be midway between the resonances and $p = 2$, then 5 kW of heating creates a plasma (Shot 50513029) with $I_p = 3.5$ kA, $\Delta I_f = -0.8$ kA, $W_p = 330$ J, $g = 2.8$, peak perpendicular pressure of 750 Pa, and maximum local beta of $\beta = (2\beta_\perp + \beta_{||})/3 = 21\%$. If R_{peak} moves outward closer to the 2.45 GHz resonance by 5 cm, $\beta = 23\%$; moving inward by 4 cm towards the 6.4 GHz resonance, the best-fit results in $\beta = 18\%$.

Additional details and analyses of high beta dipole-confined plasma will be presented in a longer article [24], but the transition to and from the high beta state warrants special mention in this letter. Fig. 4 shows measurements of the HEI instability at the transitions from low beta to high beta and from high beta to low beta. The frequency spectrum and mode structure of these fluctuations resemble previous observations of HEI in a dipole [15, 16]. The radial transport induced by the instability creates hysteresis in the neutral gas fueling required to maintain sufficient density to stabilize high beta plasma. When the neutral pressure in the chamber is less than a threshold then the HEI instability causes nearly continuous bursts of electrostatic fluctuations as measured with high-impedance floating potential probes (Fig. 4b). Rapid outward transport of fast electrons is observed with negatively-biased edge probes, and inward transport is observed by the target x-rays emitted as electrons impact the dipole (Fig. 2). Once the pressure threshold is exceeded, the plasma density and visible light abruptly increases and the HEI immediately stabilizes. As shown in Fig. 4a, this pressure threshold depends upon the ECRH power level. At 2 kW, the HEI is stabilized and the transition to high beta occurs at a pressure just above 2×10^{-6} Torr. At 4 kW and 5 kW, the transition pressures are 2.8 and 3.2×10^{-6} Torr. Once the plasma enters the higher density, high beta state, the high-beta electrons remain grossly stable so long as the neutral pressure remains above 1×10^{-6} Torr. When the pressure drops below the threshold (Fig. 4c), the fast electron confinement is destroyed and the plasma density and beta essentially disappear within a few msec. At high beta, the HEI fluctuations can resonate with the drift motion of electrons with high energies $E_h > 100$ keV; whereas, at low beta, the fluctuations resonate with lower-energy electrons, $E_h < 60$ keV.

In summary, stable high-beta plasma containing fast energetic electrons has been created and sustained in a laboratory dipole experiment using 5 kW of ECRH power and controlled neutral gas fueling. X-ray images show the high beta trapped electrons to be localized at the fundamental cyclotron resonance. The plasma current calculated from model anisotropic pressure profiles are fit to magnetic measurements and show the peak local beta reaches 20%. If the neutral gas fueling is insufficient, HEI instabilities either prevent the build-up of fast-electron beta or rapidly destroy fast-electron confinement.

We gratefully acknowledge the technical expertise of V. Fishman, R. Lations, J. Minervini, D. Strahan, and A. Zhukovsky. This work was supported by US DOE Grants DE-FG02-98ER54458 and DE-FG02-98ER54459.

* Electronic address: garnier@mit.edu

[1] J. Kesner, L. Bromberg, D.T. Garnier, M.E. Mauel, in *Fusion Energy 1998* (IAEA, Vienna, 1999) Vol. 3, p 1165.

[2] A. Hasegawa, Comments Plasma Phys. Controlled Fusion, **1**, (1987) 147.

[3] M.N. Rosenbluth and C.L. Longmire, Ann. Phys. **1**, (1957) 120.

[4] I.B. Bernstein, E. Frieman, M. Kruskal, R. Kulsrud, Proc. R. Soc. Lond. A **244** (1958) 17.

[5] T. Gold, J. Geophys. Res., **64** (1959) 123.

[6] D.T. Garnier, J. Kesner, M.E. Mauel, Phys. Plasmas **6**, (1999) 3431.

[7] R. A. Dandl, A. C. England, W. B. Ard, H. O. Eason, M. C. Becker, and G. M. Hass, Nuc. Fusion, **4**, 344 (1964).

[8] R. A. Dandl, F. W. Baity Jr., K. H. Carpenter, J. A. Cobble, H. O. Eason, *et al.*, Nuc. Fusion, Suppl., v 2, 355 (1979).

[9] B. H. Quon, R. A. Dandl, W. DiVergilo, G. E. Guest, L. L. Lao, *et al.*, Phys. Fluids, **28**, 1503 (1985).

[10] X. Chen, B. G. Lane, D. L. Smatlak, R. S. Post, and S. A. Hokin, Phys. Fluids B, **1** (1989) 615.

[11] N. Krall, Phys. Fluids, **9**, 820 (1966).

[12] H.L. Berk, Phys. Fluids, **19**, 1275 (1976).

[13] S. Hiroe, J. B. Wilgen, F. W. Baity, L. A. Berry, *et al.*, Phys. Fluids, **27**, 1019 (1984).

[14] M.E. Mauel, Journal de Physique, IV **7**, (1997) 307.

[15] H. P. Warren, M. E. Mauel, Phys. Rev. Lett., **74** (1995) 1351; and H. P. Warren and M. E. Mauel, Phys. Plasmas **2**, (1995) 4185.

[16] B. Levitt, D. Mastovsky, and M.E. Mauel, Phys. Plasmas **9**, (2002) 2507.

[17] D. Maslovsky, B. Levitt, and M. E. Mauel, Phys. Rev. Lett., 185001, **90** (2003).

[18] I. A. Daglis, R. M. Thorne, W. Baumjohann, and S. Orsini, Rev. Geophys., **37**, 4 (1997).

[19] S. von Goeler, S. Jones, R. Kaita, S. Bernabei, *et al.*, Rev. Sci. Instr., **65**, 1621 (1994).

[20] D. Batchelor, Nuc. Fusion **21** (1981) 1615.

[21] M. E. Mauel, Phys. Fluids, **27** (1984) 2899.

[22] S.I. Krasheninnikov and P.J. Catto, Phys. Plasmas, **7**, 626 (2000).

[23] A.N. Simakov, R. J. Hastie, and P.J. Catto, Phys. Plasmas, **7**, 3909 (2000).

[24] D. Garnier, A. Boxer, J. Ellsworth, A. Hansen, *et al.*, to be submitted to *Phys. Plasmas*.

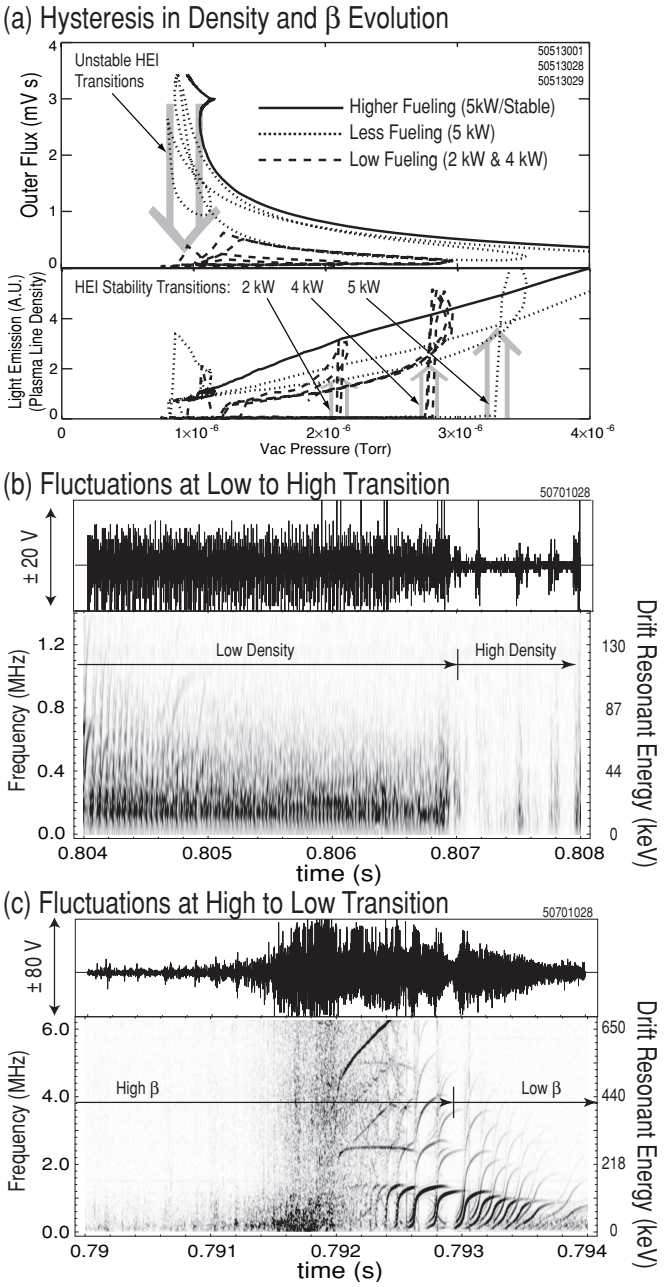

FIG. 4: Hysteresis (a) in the transitions between high beta and low-density operation caused by HEI instability (b,c). In (a), the evolution of three discharges are shown: one, with higher fueling, is always stable; two, with less fueling, have transitions to stability (at 2-3 μTorr) and unstable HEI transitions to low beta (at 1 μTorr).